

Supporting information

Photocatalytic Enhancement of Hybrid C_3N_4/TiO_2 Prepared via Ball Milling Method

Jianwei Zhou^{1,2}, Mo Zhang², and Yongfa Zhu^{2*}

1. Institute of energy and fuel, Xinxiang University, Xinxiang, China 453003, 2. Department of
Chemistry, Tsinghua University, Beijing, China 100084

Corresponding author: E-mail: zhuyf@tsinghua.edu.cn; Fax: +86-10-62787601; Tel: +86-10-
6287601

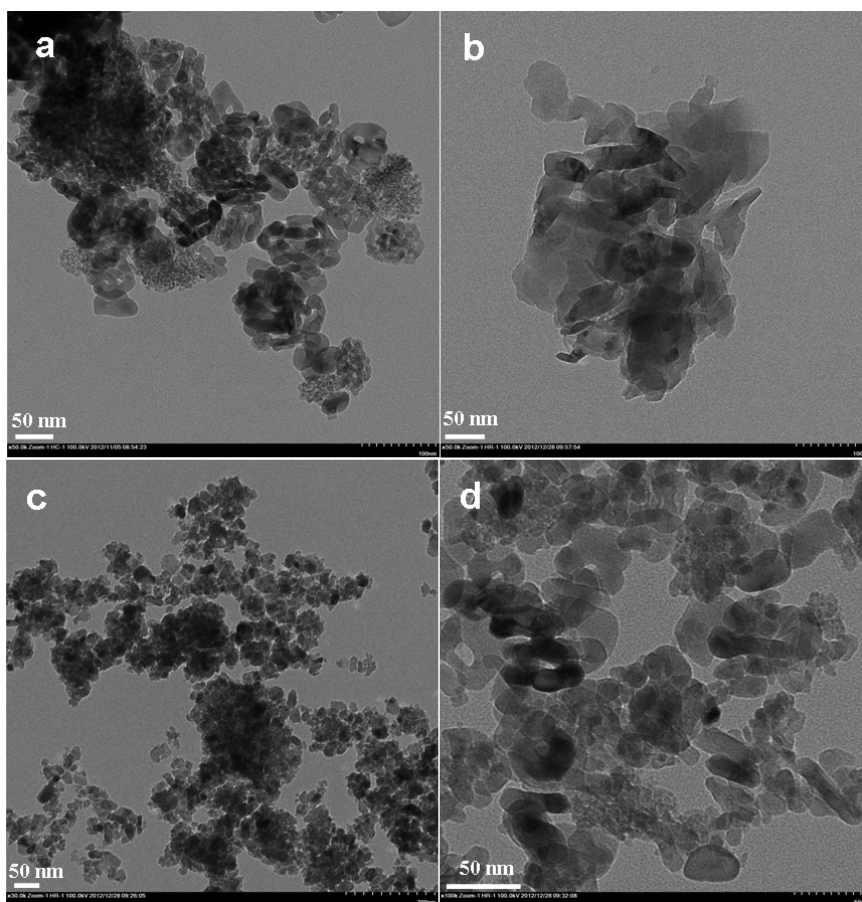


Fig. S1 TEM images of TiO₂ (a), g-C₃N₄ (b), 3%-C₃N₄/TiO₂ (c) and 5%-C₃N₄/TiO₂ (d)

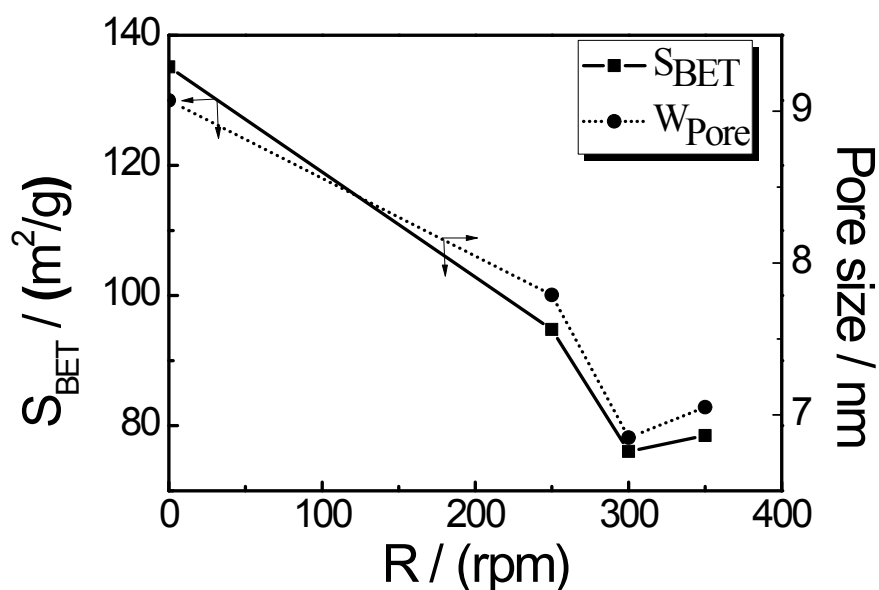


Fig.S2 Diagram of specific surface area, pore size with different ball milling speeds

Fig. S2 shows the effect of ball milling speed on the surface area and pore size of 3%-C₃N₄/TiO₂ sample. The specific surface area (S_{BET}) and pore size of C₃N₄/TiO₂ were decreased gradually with increased milling speed. The mechanical activation of materials accompanied disintegration and generation of fresh surfaces which were unexposed previously. In addition, the size distribution and the specific surface area also depend on the secondary processes like aggregation and agglomeration. The decreased surface area with increasing milling speed indicates the aggregation of particles. The inferences were verified by the TEM results of C₃N₄/TiO₂ hybrid photocatalyst.

Table 1 XPS data of the samples, the binding energies (eV) of Ti2p, O1s, N1s, and C1s

Sample	Ti2p		O1s	N1s	C1s
	Ti2p _{3/2}	Ti2p _{1/2}			
TiO ₂ *	458.60	464.40	530.02	–	–
3%-C ₃ N ₄ /TiO ₂	458.67	464.57	530.07	399.17	284.87

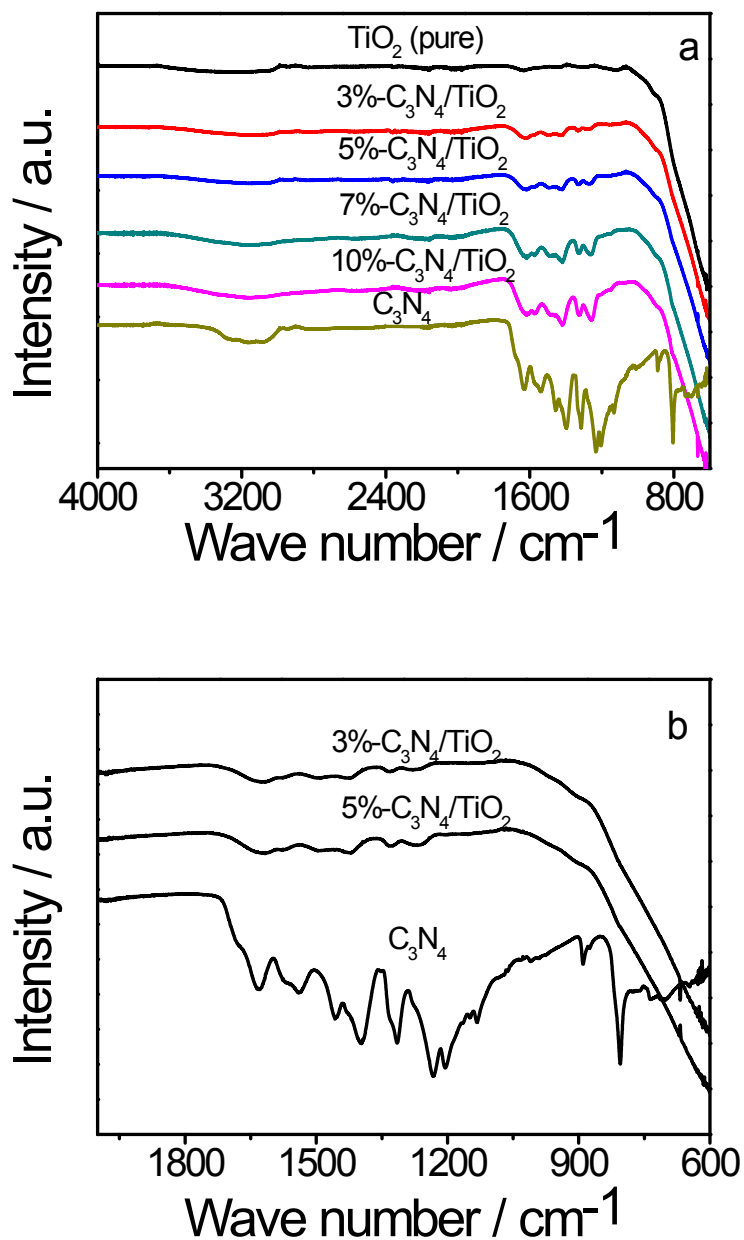


Fig. S3 FT-IR spectra of C_3N_4 , TiO_2 and $\text{C}_3\text{N}_4/\text{TiO}_2$ (A resolution of 0.5 cm^{-1})

Fig. S3a and b illustrate the FT-IR spectrum of C_3N_4 , TiO_2 and $\text{g-C}_3\text{N}_4/\text{TiO}_2$, respectively. The absorption band near 1635 cm^{-1} is attributed to C–N stretching, while the bands at 1240 , 1320 and 1405 cm^{-1} correspond to aromatic C–N stretching. The band near 810 cm^{-1} is attributed to out-of plane bending modes of C–N heterocycles^{1, 2}. A broad band near 3140 cm^{-1} corresponds to the stretching modes of terminal NH_2 or NH groups at the defect sites of the aromatic ring³. All the FT-IR

peaks can be ascribed to g-C₃N₄. The IR spectra of g-C₃N₄/TiO₂ are similar to those of C₃N₄. With the increased amount of g-C₃N₄ loading, the absorbance band intensity of g-C₃N₄/TiO₂ is gradually increased, which indicates the formation of composite between TiO₂ and C₃N₄. The stronger valence bond interaction between C₃N₄ and TiO₂ may be the main factor to the enhanced photocatalytic activity.

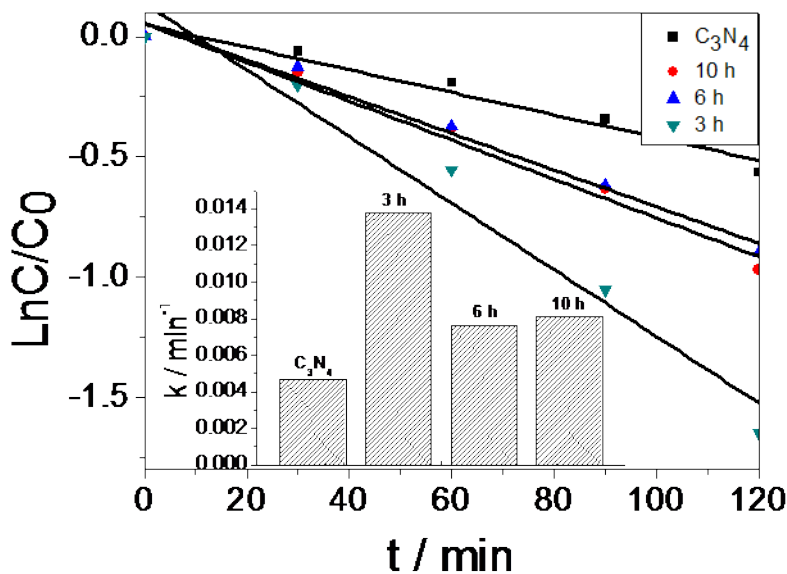


Fig. S4 Effects of ball milling time on the photocatalytic activities under visible light

The effect of ball milling time on the photocatalytic activities of g-C₃N₄/TiO₂ photocatalysts are shown in Fig. S4. It can be seen that the photocatalytic activity are influenced strongly by ball milling time. The optimum milling time is 3 h. When ball milling time is longer than 3 h, the photocatalytic activity decreases gradually with the increase of ball milling time. And the reaction rate of g-C₃N₄/TiO₂ with milling time of 3 h is about 2 times as that of 10 h. The result is mainly caused by the increased activity sites and crystal lattice distortion of TiO₂ in the ball milling process.

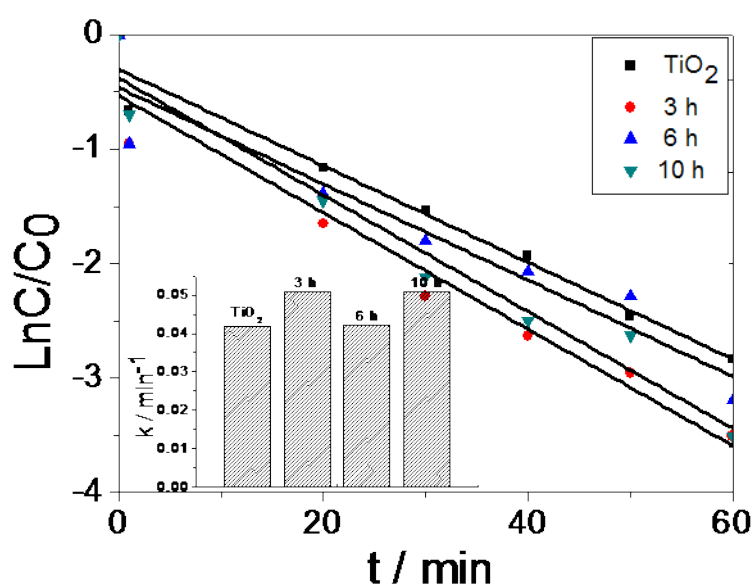


Fig. S5 The influence of different ball milling time on photocatalytic activity under UV light

After ball milling for 3 h, the activity of 3%-C₃N₄/TiO₂ is 1.2 times as pure TiO₂. The UV activity of C₃N₄/TiO₂ is enhanced via mechanochemical milling, indicating the hybrid structure of C₃N₄/TiO₂ materials. With the increase of ball milling time, the number of photocatalytic active sites is also increased. When the ball milling time is longer than the optimum time (3h), the fresh surfaces formed by high-energy ball milling possess prefer to agglomerate.

Table S1 The specific surface area (S_{BET}) pore volume (V_p), and average pore diameter of the samples at different milling speed and with different C₃N₄ loading.

Samples	TiO ₂	1%	3%			5%	7%	10%
		350 rpm	250 rpm	300 rpm	350 rpm	350 rpm	350 rpm	350 rpm
S _{BET} (m ² /g)	135	94.6	74.8	76.0	78.5	69.2	31.7	27.6
Pore volume (cm ³ /g)	0.29	0.15	0.11	0.11	0.11	0.12	0.06	0.06
Average pore diameter (nm)	8.53	6.43	5.75	5.64	5.67	6.79	7.99	8.45

As shown in Table S1, the value of S_{BET} increased with increase of milling speed and decreased gradually with increased C_3N_4 loading, indicating that the surface area of $\text{C}_3\text{N}_4/\text{TiO}_2$ increased significantly after ball milling. However, when coating with C_3N_4 , the S_{BET} of TiO_2 decreased obviously, which may due to the agglomeration of $\text{C}_3\text{N}_4/\text{TiO}_2$ with increasing C_3N_4 loading.

References

- 1 S. C. Yan, Z. S. Li, Z. G. Zou, *Langmuir*. 2009, 25, 10397-10401.
- 2 Y. J. Zhang, A. Thomas, M. Antonietti, X. C. Wang, *J. Am. Chem. Soc.* 2009, 131, 50-52.
- 3 L. Liu, D. Ma, H. Zheng, X. J. Li, M. J. Cheng, X. H. Bao, *Microporous Mesoporous Mater.* 2008, 110, 216-222.